

## Hydrogenic impurity states in a quantum well: A simple model

G. Bastard

*Groupe de Physique des Solides de l'École Normale Supérieure, \* 24 rue Lhomond, 75231 Paris Cedex 05, France*

(Received 3 November 1980)

A variational calculation of hydrogenic impurity states in a quantum well has been performed. The binding energy of donor (acceptor) levels is calculated as a function of layer thickness and of the impurity position. It is found that the ground impurity state degeneracy with respect to the impurity position is lifted, leading to the formation of some sort of an "impurity band." The density of states of this impurity band exhibits one or two peaks energetically located at the "band" extrema. This one-dimensional feature can be evidenced in the optical absorption associated with valence subband→donor transitions, whereas acceptor→conduction processes are almost featureless. In the case of conduction→acceptor luminescence a smooth curve is obtained for degenerate electronic distribution, whereas nondegenerate electron→trapped hole recombination spectra should again exhibit a double peak.

### I. INTRODUCTION

The recent advance of molecular beam epitaxy has made possible the growth of tailored semiconductors in which the band edges exhibit an oscillatory variation with the position. These new one-dimensional periodic structures, the superlattices, first proposed by Esaki and Tsu,<sup>1</sup> have recently attracted considerable attention. The GaAs-GaAlAs structures are, by far, the most simple superlattices.<sup>2</sup> Except for transport properties where the use of coupled wells is crucial,<sup>14</sup> the tight-binding approximation that leads to essentially zero bandwidth along the superlattice direction is quite adequate for explaining the majority of the experiments. InAs-GaSb superlattices are more complicated but offer a wider range of interest.<sup>3,4</sup> Electrons and holes are to a large extent spatially separated; semimetallic structures can be built from two semiconducting materials, etc. In both types of superlattices the free-electron properties seem to be well understood. In particular, steplike optical-absorption spectra between conduction and valence subbands have been observed,<sup>2</sup> strongly supporting the model of a two-dimensional character of the carrier in the superlattice planes.

Recent luminescence experiments performed by Voisin *et al.*<sup>5</sup> in InAs-GaSb superlattices exhibit a structure energetically located below the intersubband free-carrier recombination line. Its intensity strongly depends on temperature. We think that such an experiment raises the question of the nature of the impurity levels in superlattices. This subject has not as yet been studied, although related problems have already been solved. Lipari<sup>6</sup> has solved the impurity problem for impurities located near oxide-semiconductor interfaces. More recently, Keldysh<sup>7</sup> studied the binding energy of Coulombic impuri-

ties in thin semiconductor slabs, where the film dielectric constant is much larger than that of the substrate. In the specific case of superlattices, the dielectric constants of parent materials (e.g., GaAs and GaAlAs) are very similar and consequently Keldysh's approximations do not apply. Finally, Combescot and Benoit à la Guillaume<sup>8</sup> discussed electron-hole droplets in superlattices having interface defects.

In this paper, we propose a first step towards understanding the hydrogenic impurity in superlattices using a variational procedure. We will limit our purpose to the simplest existing superlattices, i.e., those which can be considered as a set of independent quantum wells. We then expect to reasonably describe the situation prevailing in GaAs-GaAlAs materials. As for the InAs-GaSb superlattices our calculations apply only to the hydrogenic acceptor states attached to the heavy-hole subbands. In fact the InAs (electron) and GaSb (light hole) levels strongly hybridize to give rise to relatively wide superlattice bands: Typically the bandwidth of the ground ( $E_1$ ) conduction subband is  $\sim 41$  meV for 50–30 Å GaSb-InAs superlattice. But a large bandwidth is equivalent to an electron wave function which is appreciably delocalized over the whole GaSb-InAs unit cell. It is therefore doubtful that the hydrogenic donor levels are well described by our independent quantum well approximation.

On the other hand, the heavy-hole superlattice bands  $H_n$  are almost dispersionless [the ground ( $H_1$ ) heavy-hole bandwidth is much less than 1 meV for a 50–30 Å GaSb-InAs superlattice]. This is due to the large (0.41 eV) energy difference separating the heavy-hole states of the two host materials and to the lack of hybridization (due to the symmetry mismatch) between the GaSb (heavy hole) and the InAs (electron) states. Hence,

the independent quantum well approximation is expected to work reasonably well to describe these InAs-GaSb heavy-hole superlattice bands and the hydrogenic acceptor states which are attached to the heavy-hole bands.

The paper is organized as follows. In Sec. II, we will derive the spectrum of ground impurity states in the independent quantum well approximation, whereas Sec. III will be devoted to the calculations of some optical properties (absorption and luminescence) associated with these bound states.

## II. SHALLOW IMPURITY LEVEL IN A QUANTUM WELL

If for simplicity one assumes that there are practically no tunneling effects between the equivalent wells of a superlattice (as, e.g., in GaAs-GaAlAs materials), that image forces are negligible, and that the carrier kinematics in one well is described by a one-band spherically symmetric effective-mass Hamiltonian, the one-impurity problem to be solved is described by the Hamiltonian

$$\mathcal{H} = \frac{p^2}{2m^*} - \frac{e^2}{\kappa[\rho^2 + (z - z_i)^2]^{1/2}} + V(z), \quad (1)$$

where  $V(z)$  is the potential-energy barrier which confines the carrier in the well. In all that follows we shall assume  $V(z)$  to be given by

$$V(z) \begin{cases} = + & \text{if } |z| > L/2, \\ = 0 & \text{if } |z| < L/2, \end{cases} \quad (2)$$

where  $L$  is the layer thickness and the  $z$  origin

$$\langle \vec{r} | \psi \rangle = \begin{cases} N \cos k_1 z \exp\left(-\frac{1}{\lambda} [\rho^2 + (z - z_i)^2]^{1/2}\right) & \text{if } |z| \leq L/2 \\ 0 & \text{if } |z| \geq L/2, \end{cases} \quad (6)$$

where  $\lambda$  is the variational parameter and  $N$  a normalization coefficient such that

$$N^2(\lambda, L, z_i) = \frac{2}{\pi \lambda^3} \left[ 1 - \cosh \frac{2z_i}{\lambda} \exp\left(-\frac{L}{\lambda}\right) + \frac{\cos 2k_1 z_i}{(1 + k_1^2 \lambda^2)^2} + \left( \frac{1}{[1 + (k_1 \lambda)^2]^2} - \frac{L}{2\lambda} \frac{k_1^2 \lambda^2}{1 + k_1^2 \lambda^2} \right) \exp\left(-\frac{L}{\lambda}\right) \cosh \frac{2z_i}{\lambda} + \frac{k_1^2 \lambda^2}{1 + k_1^2 \lambda^2} \frac{z_i}{\lambda} \sinh \frac{2z_i}{\lambda} \exp\left(-\frac{L}{\lambda}\right) \right]^{-1}. \quad (7)$$

Denoting by  $\epsilon(L, z_i)$  the eigenenergies of (1), the binding energy  $E(L, z_i)$  will be equal to

$$E(L, z_i) = \frac{\hbar^2}{2m^*} \frac{\pi^2}{L^2} - \epsilon(L, z_i). \quad (8)$$

As may be seen from Eqs. (6) and (7), our trial wave function is an exact solution of the Hamiltonian (1) in both limits  $L = 0$  and  $L = \infty$ .

is chosen at the center of the well. In Eq. (1),  $m^*$  is the carrier effective mass and  $\kappa$  the dielectric constant of the material of interest.  $\rho^2 = x^2 + y^2$  is the distance in the layer plane measured from the impurity site and  $z_i$  the coordinate of the impurity site along the superlattice axis (i.e., perpendicular to the layer plane). We have assumed that the surface layer is sufficiently large to be able to choose the  $(x, y)$  origin at the impurity site. For the sake of definiteness, we will only refer to donor level, whereas it is clear that (1) also applies to the acceptor state provided  $\mathcal{H}$  is understood as the hole Hamiltonian.

Without the impurity potential, the eigenstates of (1) are

$$\langle \vec{r} | n \vec{k}_1 \rangle \begin{cases} \left( \frac{2}{LS} \right)^{1/2} e^{i \vec{k}_1 \cdot \vec{r}} \cos k_n z, & n \text{ odd} \\ \left( \frac{2}{LS} \right)^{1/2} e^{i \vec{k}_1 \cdot \vec{r}} \sin k_n z, & n \text{ even} \end{cases} \quad (3)$$

where  $S$  is the layer surface,  $\vec{k}_1 = (k_x, k_y)$ , and

$$k_n = n\pi/L, \quad n \geq 1. \quad (4)$$

The eigenenergies corresponding to the wave function (3) are

$$\epsilon_{n \vec{k}_1} = \frac{\hbar^2 k_1^2}{2m^*} + \frac{\hbar^2 k_n^2}{2m^*}. \quad (5)$$

Because the transverse and longitudinal variables ( $\rho, z$ ) do not separate, Eq. (1) probably cannot be solved exactly. We have therefore attempted a variational solution of Eq. (1) with the trial wave function

For  $L = \infty$  and  $z_i = 0$ , Eq. (6) reduces to the ground state of the three-dimensional hydrogen atom:

$$\langle \vec{r} | \psi \rangle = (\pi \lambda^3)^{-1/2} \exp\left(-\frac{1}{\lambda} (\rho^2 + z^2)^{1/2}\right)$$

with

$$\lambda = a_0^* = \kappa \hbar^2 / m^* e^2 \quad (9)$$

and

$$E(\infty, 0) = R_0^* = m^* e^4 / 2\kappa^2 \hbar^2,$$

whereas if  $z_i = \pm L/2$  and  $L \rightarrow \infty$ , the  $2p_x$  hydrogenated state is obtained, in agreement with Levine's result<sup>9</sup>

$$\lim_{L \rightarrow \infty} E(L, \pm L/2) = \frac{1}{4} R_0^*. \quad (10)$$

For  $L = 0$ , the expression (6) reduces to the ground state of the two-dimensional hydrogen atom<sup>10</sup>

$$\langle \vec{\rho} | \psi \rangle = \left( \frac{2}{\pi \lambda^2} \right)^{1/2} \exp\left(-\frac{\rho}{\lambda}\right) \quad (11)$$

$$\epsilon(L, z_i) = \frac{\hbar^2 k_1^2}{2m^*} + \frac{\hbar^2}{2m^* \lambda^2} - \frac{e^2 \pi N^2 \lambda^2}{2\kappa} \left[ 1 + \frac{\cos(2k_1 z_i)}{1 + k_1^2 \lambda^2} - \frac{k_1^2 \lambda^2}{1 + k_1^2 \lambda^2} \exp\left(-\frac{L}{\lambda}\right) \cosh\left(\frac{2z_i}{\lambda}\right) \right]. \quad (14)$$

Extremalizing  $\epsilon(L, z_i)$  with respect to  $\lambda$ , one obtains the binding energies  $E(L, z_i)$  as a function of the layer thickness for a given  $z_i$ , or as a function of the impurity position  $z_i$  along the superlattice axis for a given thickness  $L$ . Figure 1 shows the variations of  $E(L, 0)$  and  $E(L, \pm L/2)$  with  $L/a_0^*$ . The binding energies are decreasing functions of the layer thickness, reaching, respectively,  $R_0^*$  and  $R_0^*/4$  in the infinite thickness limit. It may be noted that the tendency to a two-dimensional behavior [i.e.,  $E(L, z_i)$  closer to  $4R_0^*$  than to  $R_0^*$ ] disappears very quickly; for  $L/a_0^* = 1$  there is already  $E(L, 0) = 2.25R_0^*$ .

Figure 2 illustrates the  $z_i$  dependence of the reduced binding energies  $E(L, z_i)/E(L, 0)$  for several

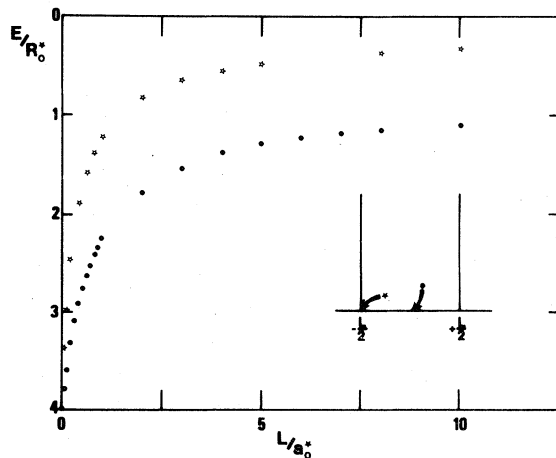


FIG. 1. Reduced binding energy versus reduced layer thickness for an impurity located at the center (dots) or at the boundary (stars) of the well.

with

$$\lambda = \frac{\kappa \hbar^2}{2m^* e^2} = \frac{a_0^*}{2}$$

corresponding to a binding energy

$$\lim_{L \rightarrow 0} E(L, z_i) = 4R_0^*. \quad (12)$$

Finally, our choice of  $\psi_{\text{trial}}(\vec{r})$  is one of the simplest which is compatible with the perfect confinement requirement

$$\psi_{\text{trial}}(\pm L/2) = 0. \quad (13)$$

With the trial wave function [Eq. (6)]  $\epsilon(L, z_i)$  can be obtained in a closed form

values of  $L/a_0^*$ . As dictated by symmetry requirements,  $E(L, z_i) = E(L, -z_i)$ .  $E(L, z_i)$  is maximum if the impurity is located at the center of the well and reaches its minimal value if  $z_i = \pm L/2$ . At this stage one may wonder whether the quantities  $E(L, z_i)$ ,  $|z_i| > L/2$  have any meaning. In fact, they correspond to bound donor levels created by donor impurities outside the well. For instance, in the specific case of GaAs-GaAlAs materials, it is possible for donors located within a GaAlAs layer to catch an electron in the neighboring GaAs layer, a problem of some interest for modulation-doping materials.<sup>11</sup> The donor wave function will be exceedingly small in the GaAlAs layer (it is a deep donor level with respect to the GaAlAs band edge), but still substantial in the GaAs layer provided  $|z_i - L/2|$  is not too large. The position dependence of this

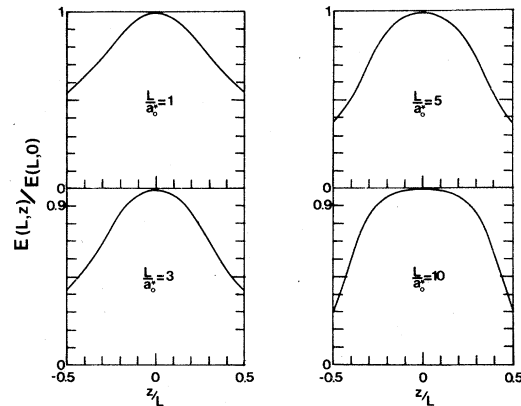


FIG. 2. Position dependence of the impurity binding energy for several layer thicknesses.

kind of donor state can be calculated within the above framework if one assumes that the energy difference between the GaAs and GaAlAs band edges is infinite [in practice much larger than  $E(L, z_i)$ ]. For  $|z_i| > L/2$ ,  $E(L, z_i)$  goes rapidly to zero: Only donors which are closer to the interface than  $a_0^*$  have an appreciable binding (Fig. 3). It should be stressed that these states are the only bound ones. The shallow donor levels which are attached to the GaAlAs band edge (and are true bound states in the absence of GaAlAs-GaAs interfaces) are, in the presence of GaAs wells, degenerate with the two-dimensional continuum of GaAs subband states. Hence they are resonant levels with a finite width and cannot trap a carrier.

In contrast with homogeneous materials, the confinement effect leads to a spreading of donor levels which depends upon the impurity position. Instead of obtaining a single ground donor level that is degenerate with respect to the impurity site, one obtains as many levels as possible of impurity coordinates along the superlattice axis. In discussing which  $L/a_0^*$  ratio leads to the largest effective spreading of the donor level, it is of interest to evaluate  $g_L(E_i)$ , which is the density of impurity states per unit binding energy. Strictly speaking, impurities are supposed to be substitutional, and if  $d$  denotes the lattice spacing there are only  $L/d + 1$  possible impurity positions  $z_i$  in the layer (we do not consider the case of modulation-doped materials here).  $g_L(E_i)$  then reduces to a sum of  $L/d + 1$  delta functions. If, however, the layer is not too thin ( $L/d \gg 1$ ), one may let  $z_i$  become a continuous random variable (if there is no intentional doping).

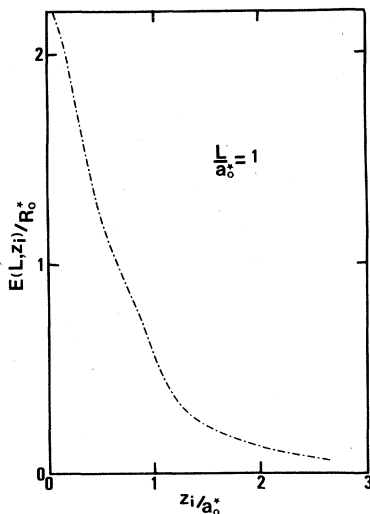


FIG. 3. Position dependence of the impurity binding energy when the impurity stays outside the well ( $L/a_0^* = 1$ ).

In this case

$$g_L(E_i) = \frac{2}{L} \left| \frac{dz_i}{dE_i} \right|, \quad E_i = E(L, z_i), \quad z_i \geq 0. \quad (15)$$

Now  $dE_i/dz_i$  vanishes at the center of the well. Also, as may be seen in Fig. 2,  $E(L, z_i)$  has a very small slope near  $z_i = \pm L/2$  if  $L/a_0^* \approx 1$ . Hence  $g_L(E_i)$  becomes infinite at  $E_i = E_{\max}^i = E(L, 0)$  and can be quite large in the vicinity of  $E_{\min}^i = E(L, \pm L/2)$  (Fig. 4). However, when  $L/a_0^*$  becomes large, the  $E_{\min}^i$  relative maximum disappears, whereas the strength of the  $E_{\max}^i$  singularity is reinforced until, for infinite thicknesses, one obtains

$$\lim_{L \rightarrow \infty} g_L(E_i) = \delta(E_i - R_0^*), \quad (16a)$$

the interface value  $E_i = E_{\min}^i = R_0^*/4$  having a negligible weight. When the well thickness decreases the  $E(L, z_i)$  curves flatten. The two singularities at  $E_{\min}^i$  and  $E_{\max}^i$  become of equivalent strength and

$$\lim_{L \rightarrow 0} g_L(E_i) = \delta(E_i - 4R_0^*). \quad (16b)$$

Qualitatively, the region  $L/a_0^* \approx 1$  realizes the maximum effective-donor spreading: The width of the donor distribution is still substantial and  $g_L(E_i)$  has two maxima.

To summarize, by changing the single eigenvalue spectrum of a donor ground state into a quasicontinuum, the spatial confinement in the well acts as if there were an impurity band. In contrast with the standard impurity band, we are dealing here with a one-impurity effect. Our results are then independent of the donor concentration (if low enough). The width  $\delta = E_{\max}^i - E_{\min}^i$  of this "impurity band" depends on the layer thick-

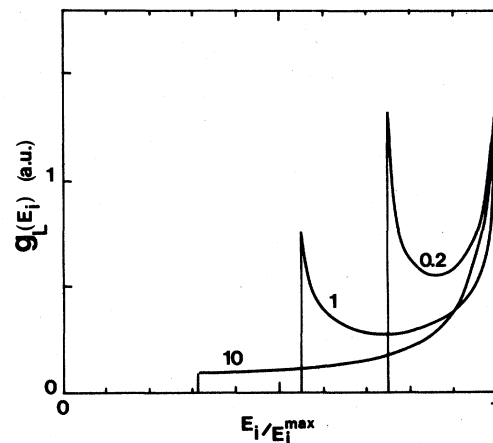


FIG. 4. Density of states  $g_L(E_i)$  vs  $E_i/E_{\max}^i$  for three layer thicknesses  $= L/a_0^* = 0.2, 1, 10$ .

ness vanishing in both limits  $L=0$ ,  $L=\infty$ . Whereas the density of states of the impurity band in doped semiconductors shows a maximum near the band center, in our case we obtain instead one or two maxima which take place near the band boundaries. From the previous analysis we expect the well thickness to sensitively affect the transport properties in the exhaustion regime, the apparent donor activation energy being  $L$  dependent in two ways: in an explicit one through  $E(L, z_i)$  and in an implicit one through  $g_L(E_i)$ . Moreover, as we shall see below, under favorable circumstances, the two density-of-states singularities may be revealed in the optical properties associated with impurities.

### III. OPTICAL PROPERTIES ASSOCIATED WITH IMPURITIES

In the preceding paragraph, we have developed a simple model for hydrogenic impurities confined between two planes. We found that the degeneracy with respect to the impurity position of the donor ground state was lifted. We are now interested in calculating the optical properties associated with such impurities. We will focus our attention on interband processes, since they are the most efficient tools to evidence donor or acceptor ground states. Absorption or emission experiments are possible. In all that follows, we shall assume that bound electron (hole) statistics play no part. This assumption is by no means crucial. It simply renders the algebra a little less involved.

Up to now we have assumed that the impurity levels were built from states belonging to a single parabolic band. This is an excellent approximation for donor levels but questionable for acceptor states. The situation is, however, better in our case than in infinite homogeneous materials. For the cubic materials of interest, the valence band is fourfold degenerate with  $J=\frac{3}{2}$  symmetry

at  $k=0$  in infinite media. The acceptor wavefunctions are correspondingly complicated. Owing to the spatial confinement, the light- or heavy-hole-band degeneracy is lifted, the upper subbands being heavy-hole-like. Then, to some extent, we are again dealing with a single-band problem. Therefore, although not entirely justified, we shall use the same model for acceptor level as for donor states.

#### A. Band $\leftrightarrow$ impurity absorption spectra

However, the problems of upper valence subband-donor state and acceptor state-lower conduction subbands are not entirely equivalent. For all materials of interest (GaAs-GaAlAs or InAs-GaSb superlattices), the effective-mass ratio  $m_{val}/m_{cond}$  is much larger than 1 (5-6 for GaAs-GaAlAs compounds and 20 for InAs-GaSb materials being typical values). As it is well known,<sup>12</sup> this asymmetry leads, for homogeneous materials, to the impossibility of observing any structure associated with acceptor-conduction-band transition by means of absorption measurements, since the impurity peak would occur at energies larger than the interband threshold.<sup>13</sup> On the other hand, valence-donor transitions can produce an absorption peak below the energy gap. Similar effects are obtained in our case. Consider first the transitions associated with a single impurity located in the plane  $z=z_i$ . Assume the interband optical transition to be allowed in the corresponding homogeneous infinite materials (the actual case in existing superlattices). The transition probability per unit time is then proportional to the square of the overlap integral between the envelope wave functions of the initial and final states. These are labeled on Table I. We have assumed that electrons and holes are in the same layer. Summing over the initial and final states and restricting ourselves to the first hole subband, one obtains

TABLE I. Wave functions and energies involved in band  $\rightarrow$  impurity transitions. The energy gap  $\epsilon_g$  includes the quantized kinetic energies of the parallel motion for electrons and holes.

First valence subband $\rightarrow$ donor	Acceptor $\rightarrow$ first conduction subband
$\langle \tilde{F} i \rangle = \left(\frac{2}{LS}\right)^{1/2} \cos(k_1 z) \exp(i \vec{k}_1 \cdot \vec{\rho})$	$\langle \tilde{F} i \rangle = N(L, z_i, \lambda) \cos(k_1 z) \exp\left(-\frac{1}{\lambda} [\rho^2 + (z - z_i)^2]^{1/2}\right)$
$\langle \tilde{F} f \rangle = N(L, z_i, \lambda) \cos(k_1 z) \exp\left(-\frac{1}{\lambda} [\rho^2 + (z - z_i)^2]^{1/2}\right)$	$\langle \tilde{F} f \rangle = \left(\frac{2}{LS}\right)^{1/2} \cos(k_1 z) \exp(i \vec{k}_1 \cdot \vec{\rho})$
$\epsilon_i = -\epsilon_g - \hbar^2 k_1^2 / 2m_v$	$\epsilon_i = -\epsilon_g + E_a(L, z_i)$
$\epsilon_f = -E_d(L, z_i)$	$\epsilon_f = \hbar^2 k_1^2 / 2m_c$

$$\tau_{\text{val-don}}^{-1}(z_i, \omega) = AN^2(L, z_i, \lambda) m_{\text{val}} J^2\left(z_i, \lambda, \left(\frac{2m_v}{\hbar^2} [\hbar\omega - \epsilon_g + E(L, z_i)]\right)^{1/2}\right) Y(\hbar\omega - \epsilon_g + E(L, z_i)), \quad (17)$$

where  $Y(t)$  is the step function

$$Y(t) = \begin{cases} 1 & \text{if } t > 0 \\ 0 & \text{otherwise.} \end{cases} \quad (18)$$

In the frequency range of band  $\rightarrow$  impurity transitions,  $A$  is an almost frequency-independent constant.  $N$  is the normalization coefficient defined in Eq. (7). In terms of the auxiliary functions

$$\alpha(x) = (x^2 + \lambda^{-2})^{1/2}, \quad (19)$$

$$\nu(x) = 2\pi/L\alpha(x), \quad (20)$$

$J$  is given by

$$J(z_i, \lambda, x) = \frac{1}{\lambda\alpha^4} \left[ 2 + \frac{2 \cos(k_z z_i)}{(1 + \nu^2)^2} + \frac{z_i \alpha \nu^2}{1 + \nu^2} \exp\left(-\frac{L\alpha}{2}\right) \sinh(\nu z_i) + \cosh(\nu z_i) \exp\left(-\frac{L\alpha}{2}\right) \left( -\frac{\nu^2 L\alpha}{2(1 + \nu^2)^2} + \frac{2}{(1 + \nu^2)^2} - 2 \right) \right]. \quad (21)$$

The case of acceptor  $\rightarrow$  first conduction subband transition is obtained by changing  $m_{\text{val}}$  into  $m_{\text{cond}}$  in Eqs. (17)–(21).

Let us stress that  $J(z_i, \lambda, 0)$  is nonvanishing. Therefore  $\tau_{\text{val-don}}^{-1}$  is a step function near the threshold  $x=0$ . This contrasts with homogeneous infinite materials for which  $\tau_{\text{val-don}}^{-1}$  and thus the absorption behaves like  $x$  near  $x=0$ . In both cases the low- $x$  behavior reflects the density of states of the initial state: In a quantum well the density of states of each valence subband is a step function characteristic of the two-dimensional motion in the layer plane.

To illustrate the asymmetry between the absorption associated with donors and acceptors, let us get rid of the cumbersome  $z_i$  dependence and assume for a while that  $L=0$  (purely two-dimensional problem). Then

$$\begin{aligned} E(L, z_i) &= 4R_{0d}^* \alpha, \\ \lambda &= \frac{1}{2} a_{0d}^* \alpha, \end{aligned} \quad (22)$$

and

$$\tau_{\text{val-don}}^{-1} \approx \frac{m_v Y(\hbar\omega - \epsilon_g + 4R_{0d}^* \alpha)}{\left(1 + \frac{1}{4R_{0d}^*} \frac{m_{\text{val}}}{m_{\text{cond}}} (\hbar\omega - \epsilon_g + 4R_{0d}^* \alpha)\right)^3}$$

whereas  $\tau_{\text{acc-cond}}^{-1}$  is obtained from (22) by changing  $m_{\text{cond}}$  into  $m_{\text{val}}$  and  $R_{0d}^*$  into  $R_{0a}^*$ . Owing to the large ratio  $m_{\text{val}}/m_{\text{cond}}$ ,  $\tau_{\text{val-don}}^{-1}$  is a fairly rapidly decreasing function of  $\hbar\omega$  above the threshold, whereas  $\tau_{\text{acc-cond}}^{-1}$  remains almost constant (Fig. 5). Hence, as in infinite materials, absorption peaks below the interband threshold can be observed in the case of valence  $\rightarrow$  donor transitions. On the other hand, acceptor  $\rightarrow$  conduction subband transitions lead only to a step in absorption.

In spite of the intricate  $z_i$  dependence exhibited by  $\tau_{\text{val-don}}^{-1}$  and  $\tau_{\text{acc-cond}}^{-1}$ , the dissymmetry between

the two kinds of absorptive processes, exhibited in Eq. (22) for  $L=0$ , is preserved. To each  $z_i$  are associated a given  $\lambda$  and a given  $E(L, z_i)$ . These were calculated and discussed in Sec. II. To obtain the frequency-dependent  $\tau^{-1}$  we have to sum expression (17) over all possible  $z_i$ , each of the  $\tau^{-1}(\omega, z_i)$  being eventually weighted by a doping profile function. If we again assume that the layer thickness is much larger than the lattice spacing and that impurities are randomly distributed, we have

$$\tau_L^{-1}(\omega) = \frac{2Am_{\text{val}}}{L} \int_0^{L/2} dz_i \tau^{-1}(z_i, \omega) \quad (23)$$

or equivalently

$$\tau_L^{-1}(\omega) = Am_{\text{val}} \int_{E_{\text{min}}^i}^{E_{\text{max}}^i} dE_i \tau^{-1}(z(E_i), \omega) g_L(E_i). \quad (24)$$

Since  $g_L(E_i)$  is singular near  $E_{\text{max}}^i$  and shows a maximum near  $E_{\text{min}}^i$  (if  $L/a_0^* \lesssim 1$ ) we may expect that, being multiplied by a sharply peaked func-

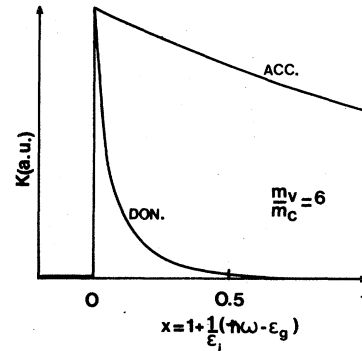


FIG. 5. Absorption coefficient (in arbitrary units) versus a dimensionless energy  $x$ . The curves labeled by don and acc correspond to valence subband  $\rightarrow$  donor and acceptor  $\rightarrow$  conduction subband, respectively.  $L=0$  (purely two-dimensional material) and  $m_{\text{val}}/m_{\text{cond}}=6$ .

tion of the argument  $\hbar\omega - \epsilon_g + E_i$ , there will result for  $\tau_L^{-1}(\omega)$  two maxima located near

$$\begin{aligned}\hbar\omega_{\min} &= \epsilon_g - E_{\max}^i, \\ \hbar\omega_{\max} &= \epsilon_g - E_{\min}^i.\end{aligned}\quad (25)$$

Therefore, due to a confinement effect, valence  $\rightarrow$  donor transitions are characterized by a double peak occurring below the interband threshold. The energy distance between these two peaks gives a direct evaluation of the confinement-induced spreading of donor ground states.

To illustrate these features we show in Fig. 6 the frequency dependence of  $\tau_{\text{val} \rightarrow \text{don}}^{-1}$  calculated from Eq. (23) for several layer thicknesses. The quantity plotted on the horizontal axis is related to  $\omega$  by

$$\hbar\omega = \epsilon_g - E_{\max}^i + xE_{\max}^i. \quad (26)$$

All curves exhibit a peak very near  $x=0$ . For  $L/a_0^* \lesssim 1$  there exists a second peak between  $x=0$  and  $x=1$ . It may be seen from Fig. 4 that the location of the second peak is

$$x_{\max} = (E_{\max}^i - E_{\min}^i)/E_{\max}^i. \quad (27)$$

In agreement with the discussion of Sec. I, the strength of the  $x_{\max}$  peak weakens as  $L/a_0^*$  increases. For  $L/a_0^* = 10$  it has disappeared.

As for acceptor  $\rightarrow$  conduction-band transitions, we previously argued that  $\tau_{\text{acc} \rightarrow \text{cond}}^{-1}(\omega, z_i)$  were almost step functions of the argument  $\hbar\omega - \epsilon_g + E_i$ . Therefore  $\tau_{\text{acc} \rightarrow \text{cond}}^{-1}$ , if considered as a function of  $x$ , should first increase with  $x$  corresponding to the successive onsets of acceptor  $\rightarrow$  conduction subband transitions [from the deepest

acceptor ( $x=0$ ) to the highest one ( $x=x_{\max}$ )]. For  $x > x_{\max}$ ,  $\tau_{\text{acc} \rightarrow \text{cond}}^{-1}(\omega)$  should decrease very slowly. These qualitative considerations are supported by numerical calculations. Figure 7 shows the curves  $\tau_{\text{acc} \rightarrow \text{cond}}^{-1}$  versus  $x$  for several layer thicknesses. In the case of acceptor  $\rightarrow$  conduction subband transitions the confinement effect leads to a steplike absorption. By experimentally measuring the energy distance between vanishing absorption and the plateau one could, in principle, deduce the width of the acceptor band. However, in practice, this determination will be far more difficult than in the case of valence  $\rightarrow$  donor transitions.

### B. Conduction subband $\rightarrow$ acceptor luminescence

Consider a superlattice in which electrons have been optically injected into the conduction band. They will recombine with free or trapped holes. The emission spectrum  $\mathcal{L}_L(\omega)$  associated with conduction band  $\rightarrow$  acceptor transitions may, to an excellent approximation, be taken as proportional to the product of  $\tau_{\text{acc} \rightarrow \text{cond}}^{-1}$  by the electronic distribution function. Denoting by  $E_F$  the Fermi energy of the electron gas measured from the bottom of the first conduction subband, we obtain

$$\begin{aligned}\mathcal{L}_L(\omega) \propto & \int_{E_{\min}^i}^{E_{\max}^i} g_L(E_i) \tau_{\text{acc} \rightarrow \text{cond}}^{-1}(\omega, L, E_i) \\ & \times \frac{1}{1 + \exp[\beta(\hbar\omega - \epsilon_g + E_i - E_F)]}.\end{aligned}\quad (28)$$

Two cases are now possible depending on whether the electron gas is degenerate or not.

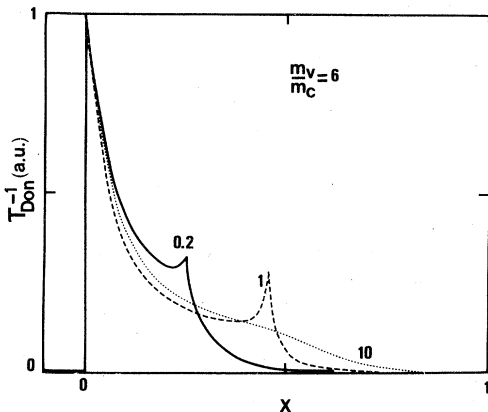


FIG. 6. Transition probability per unit time  $\tau_{\text{val} \rightarrow \text{don}}^{-1}$  corresponding to valence  $\rightarrow$  donors transitions plotted against a dimensionless frequency  $x$  [see Eq. (26)] for three layer thicknesses:  $L/a_0^* = 0.2, 1, 10$ .  $m_{\text{val}}/m_{\text{cond}} = 6$ . The three curves are scaled to reach 1 at their maxima.

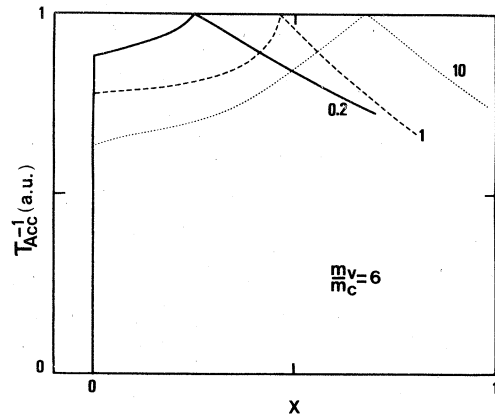


FIG. 7. Transition probability per unit time  $\tau_{\text{acc} \rightarrow \text{cb}}^{-1}$  corresponding to acceptor  $\rightarrow$  first conduction subband transitions plotted against a dimensionless frequency  $x$  [see Eq. (26)] for three layer thicknesses:  $L/a_0^* = 0.2, 1, 10$ .  $m_{\text{val}}/m_{\text{cond}} = 6$ . The three curves are scaled to reach 1 at their maxima.

## 1. Degenerate electron gas

If the electron gas is degenerate, the emission spectrum to a given acceptor characterized by  $E_i$  is roughly equal to the product of a step function of the argument  $\hbar\omega - \epsilon_g + E_i$  by another step function of the argument  $E_F - \hbar\omega + \epsilon_g - E_i$ . To see roughly which kind of luminescence spectrum results from the recombination of free electrons with trapped holes in the "acceptor band," let us approximate  $g_L(E_i)$  by a constant and  $\tau^{-1}(E_i)$  by a step function and let us assume that  $T=0$  and  $E_F/E_{\max}^i < x_{\max}$ . Then, using again the variable defined in Eq. (26), one immediately obtains

$$\Omega_L(x) \propto \begin{cases} x & \text{if } 0 \leq x \leq \frac{E_F}{E_{\max}^i} \\ \frac{E_F}{E_{\max}^i} & \text{if } \frac{E_F}{E_{\max}^i} \leq x \leq x_{\max} \\ \frac{E_F}{E_{\max}^i} - x + x_{\max} & \text{if } x_{\max} \leq x \leq x_{\max} + \frac{E_F}{E_{\max}^i} \\ \Omega_L(x) = 0 & \text{if } x_{\max} + \frac{E_F}{E_{\max}^i} \leq x. \end{cases} \quad (29)$$

Therefore the high-energy side of the luminescence line should not be used to derive the electronic temperature. Although the assumption of a constant  $g_L(E_i)$  is oversimplified, it may be seen from Fig. 8 that the luminescence line shape Eq. (29) is not, in the high- $x$  region, too bad an approximation of the one calculated from the full expression in Eq. (28). This is due to the smooth variation of  $\tau_L^{-1}(E_i)$ .

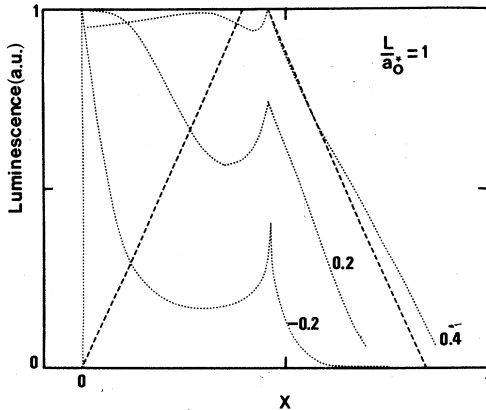


FIG. 8. Luminescence spectra associated with electron  $\rightarrow$  acceptors recombinations for three different Fermi energies:  $E_F/E_{\max}^i = -0.2, 0.2, 0.4$ .  $L/a_0^* = 1$ ,  $m_{\text{val}}/m_{\text{cond}} = 6$ . The dashed line corresponds to the approximate spectrum [see Eq. (29)]. The curves are scaled to reach 1 at their maxima.

## 2. Nondegenerate electron gas

If, on the other hand, the electron gas is nondegenerate, the emission spectrum characterizing a well-defined acceptor of the energy  $E_i$  is a sharply peaked function of the variable  $\hbar\omega - \epsilon_g + E_i$  (being the product of a step function of the same argument by the exponentially decreasing term  $\exp[-\beta(\hbar\omega - \epsilon_g + E_i)]$ ). Therefore the emission spectrum  $\Omega_L(\omega)$  of nondegenerate carriers to acceptor states should exhibit the same features as the absorption spectrum associated with valence-donor transitions. Namely, the two spectra should present a double-peak structure near  $x=0$  and  $x=x_{\max}$ , the energy distance between the two peaks giving a fair evaluation of the impurity ground state spreading by confinement effect. As an illustration of the above discussion, we show in Fig. 8 the calculated emission spectra associated with electron acceptor recombination for a given layer thickness ( $L/a_0^* = 1$ ), a given electronic temperature ( $\beta E_{\max}^i = 23$ ) and different Fermi energies.

## IV. CONCLUSION

In this paper, we have attempted a simple variational calculation of impurity levels in a quantum well. Since we have neglected any tunneling effect between equivalent wells, our calculations apply to donor or acceptor levels in GaAs-GaAlAs structures or to acceptor levels in InAs-GaSb superlattices. Even for diluted impurities, the spatial confinement effect leads to the formation of a sort of impurity band. The density of states of this "impurity band" is singular near the band extrema due to the one-dimensional character of the impurity position along the layer axis. The existence of this "impurity band" is expected to influence both the transport properties in the exhaustion regime and the optical properties associated with impurities. The valence subband  $\rightarrow$  donor absorption spectra should reflect the shape of the "donor impurity band" whereas, due to the asymmetry between the conduction and valence masses, the acceptors  $\rightarrow$  conduction subband absorption is almost featureless. The conduction subband  $\rightarrow$  acceptors luminescence is also a smooth function of the energy for degenerate electron gas, whereas nondegenerate electron recombination with trapped holes could again give some information on the width of the "acceptor band."

## ACKNOWLEDGMENTS

I would like to thank Dr. M. Voos and Dr. P. Voisin for communicating to me their results



prior to publication, and for innumerable valuable discussions on the subject of impurity states in superlattices. I am grateful to Dr. H. Serre

for considerable help in the numerical calculations, and to Dr. M. Combescot and Dr. C. Benoit à la Guillaume for helpful discussions.

---

\*Laboratoire associé au Centre de la Recherche Scientifique.

<sup>1</sup>L. Esaki and R. Tsu, I.B.M. J. Res. Dev. 14, 61 (1970).

<sup>2</sup>For a review see R. Dingle, in *Festkörperprobleme* (Advances in Solid State Physics), edited by M. J. Queisser (Pergamon-Vieweg, Braunschweig, 1975), Vol. XV, p. 21.

<sup>3</sup>G. A. Sai-Halasz, R. Tsu, and L. Esaki, Appl. Phys. Lett. 30, 651 (1977).

<sup>4</sup>G. A. Sai-Halasz, in *Proceedings of the 14th International Conference on the Physics of Semiconductors, Edinburgh, 1978*, edited by B. L. H. Wilson (Institute of Physics, London, 1978), p. 21.

<sup>5</sup>P. Voisin, Y. Guldner, J. P. Vieren, M. Voos, C. Benoit à la Guillaume, N. J. Kawai, L. L. Chang, and L. Esaki, in *Proceedings of the 15th International Conference on the Physics of Semiconductors, Kyoto, 1980* J. Phys. Soc. Jpn. 49, Suppl. A, 1005 (1980).

<sup>6</sup>N. O. Lipari, J. Vac. Sci. Technol. 15, 1412 (1978).

<sup>7</sup>L.V. Keldysh, Zh. Eksp. Teor. Fiz. Pis'ma Red. 29,

716 (1979) [JETP Lett. 29, 658 (1979)].

<sup>8</sup>M. Combescot and C. Benoit à la Guillaume, private communication and Solid State Commun. (in press).

<sup>9</sup>J. D. Levine, Phys. Rev. A 2, 586 (1965).

<sup>10</sup>W. Kohn and J. M. Luttinger, Phys. Rev. 98, 915 (1955).

<sup>11</sup>H. L. Störmer, R. Dingle, A. C. Gossard, W. Wiegmann, and R. A. Logan, in *Proceedings of the 14th International Conference on the Physics of Semiconductors, Edinburgh, 1978*, edited by B. L. H. Wilson (Institute of Physics, London, 1978), p. 557.

<sup>12</sup>D. M. Eagles, J. Phys. Chem. Solids 16, 76 (1960).

<sup>13</sup>This statement is only true for hypothetical hydrogenated acceptors attached to a nondegenerate parabolic band. If one takes care of the  $\Gamma_8$  band degeneracy for acceptor wave functions, the absorption coefficient associated with acceptor  $\rightarrow$  conduction band transitions shows a maximum below the interband threshold (C. Rigaux and G. Bastard, unpublished).

<sup>14</sup>R. Tsu and G. Döhler, Phys. Rev. B 12, 680 (1975).